Applied Catalysis B: Environmental 92 (2009) 271–279

Contents lists available at ScienceDirect

Applied Catalysis B: Environmental

journal homepage: www.elsevier.com/locate/apcatb

Selective oxidation of H_2S to sulfur over vanadia supported on mesoporous zirconium phosphate heterostructure

M.D. Soriano [a], J. Jiménez-Jiménez [b], P. Concepción [a], A. Jiménez-López [b], E. Rodríguez-Castellón [b], J.M. López Nieto [a,*]

[a] Instituto de Tecnología Química, UPV-CSIC, Avenida de los Naranjos s/n, 46022 Valencia, Spain
[b] Dep. Química Inorgánica, Facultad de Ciencias, Universidad de Málaga, 29071 Málaga, Spain

ARTICLE INFO

Article history:
Received 24 April 2009
Received in revised form 30 July 2009
Accepted 3 August 2009
Available online 8 August 2009

Keywords:
Selective oxidation
Hydrogen sulfide
Mesoporous zirconium phosphate support
Supported vanadium oxide
V_4O_9
V_2O_5

ABSTRACT

Vanadium oxide supported on mesoporous zirconium phosphate catalysts has been synthesized, characterized and tested in the selective oxidation of H_2S to sulfur. The nature of the vanadium species depends on the V-loading of catalyst. Catalysts with a V-content lower than 4wt% present both isolated vanadium species and V_2O_5 crystallites. However, V_2O_5 crystallites have been mainly observed in catalysts with higher V-content, although the presence of isolated V-species on the surface of the metal oxide support cannot be completely ruled out. The catalytic behaviour also depends on V-loading of catalysts. Thus, while the catalytic activity of catalysts can be related to the number of V-sites, the catalyst decay is clearly observed in samples with low V-loading. The characterization of catalysts after the catalytic tests indicates the presence of sulfur on the catalyst, which is favoured on catalysts with low V-loading. However, a clear transformation of V_2O_5 to V_4O_9 can be proposed according to XRD and Raman results of used catalysts with high V-loading. The importance of V^{5+}–O–V^{4+} pairs in activity and selectivity is also discussed.

1. Introduction

Hydrogen sulfide is usually removed by the well-known Claus process, a two-step process including thermal oxidation (in which one-third of the hydrogen sulfide is first burned with air to sulfur dioxide in a waste heat furnace) and catalytic reaction (in which SO_2 is reacted with unconverted H_2S to produce elemental sulfur) [1]. However, due to thermodynamic limitations, the process is limited to about 95–97%.

From a practical point of view, the most attractive way of sulfur production from hydrogen sulfide is selective oxidation by using oxygen from air, according to reaction [2–4]: $H_2S + 1/2O_2 \rightarrow H_2O + 1/x\ S_x$. However, selective catalysts are required since SO_2 can also be formed depending on reaction temperature and H_2S/O_2 ratio.

Vanadium-based catalysts have been reported to be active and selective for the partial oxidation of H_2S to sulfur in the 200–300 °C temperature range [5–19]. Although V_2O_5 is active and selective in the selective oxidation of hydrogen sulfide to elemental sulfur [5–7], other vanadium-based catalysts have been also proposed. This is the case of the use of mixed metal oxides, i.e. V–Mg–O [8], rare earth vanadates [10,11], V–Sb–O [12], Mo–V–O [8,13], Cu–V–O [14], or supported vanadium oxides [11,15,16–19]. Among these, alumina- and titania-supported vanadia catalysts have been the most studied catalysts. It is known that the characteristics of metal oxide support and the nature of vanadium species strongly influence the catalytic performance of supported vanadium catalysts. However, the nature of active and selective sites is still under discussion.

On the other hand, two important aspects must also be considered in the case of supported vanadium oxide catalysts in order to improve the catalytic performance of these catalysts: (i) catalyst deactivation and (ii) selectivity to sulfur, since SO_2 can also be formed by a competitive way. In this way, a catalyst decay could be related to the reduction of vanadium oxide (forming VO_2 or V_2O_3) [6] and/or the formation of less active forms of vanadium, as vanadyl sulfate ($VOSO_4$) [17]. Thus, the catalyst decay with time on stream could be due to a depletion of labile oxygen on the catalyst surface, which depends on both the redox properties of catalysts and the reaction conditions [6]. In addition, and depending on the reaction conditions, sulfidation of the metal and metal oxide components could also result in a low stability of the catalysts.

A mesoporous zirconium phosphate heterostructure, prepared using a synthetic strategy that combines the synthesis of pillared layer structures (PLS) and MCM-41 mesoporous solids (Fig. 1), where zirconium phosphate is expanded with the formation of silica galleries in the interlayer space, has been proposed [21]. This is an interesting material to be used as support since it shows a

* Corresponding author. Tel.: +34 963877808; fax: +34 963877809.
E-mail address: jmlopez@itq.upv.es (J.M. López Nieto).

0926-3373/$ – see front matter © 2009 Elsevier B.V. All rights reserved.
doi:10.1016/j.apcatb.2009.08.002

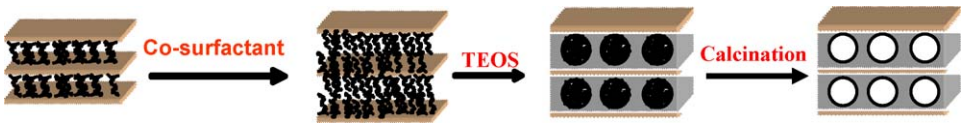

Fig. 1. Scheme of the synthesis of the mesoporous zirconium phosphate heterostructure.

high thermal stability, high surface area and acid sites which could favour a relatively high dispersion of vanadium. Moreover, it possesses also big pores in which metal oxides with relatively low crystal sizes could be formed [21].

In this paper, we present the synthesis, characterization and catalytic performance for the selective oxidation of hydrogen sulfide to sulfur of vanadium oxide supported on a mesoporous zirconium phosphate heterostructure. It will be shown that the vanadium loading influences the catalytic behaviour and how the presence of nanoparticles of V_2O_5 as precursor of the active sites favours a high activity and selectivity. The characterization of used catalysts will be used for understanding the nature of active sites.

2. Experimental

2.1. Catalyst preparation

The mesoporous zirconium phosphate heterostructure, MZP (S_{BET} = 556 $m^2\ g^{-1}$; porous diameter in the mesoporous range, i.e. 3 nm), was prepared according to a previously reported preparation procedure [21]. The solid was then centrifuged, washed with ethanol and dried at 120 °C in air. This precursor material was calcined at 550 °C for 6 h (1.5 °C min^{-1} heating rate). A scheme of the synthesis of the support is shown in Fig. 1.

Vanadium oxides supported on mesoporous zirconium phosphate (*n*V-MZP, in which *n* is the V-content in wt%) were prepared by the wet-impregnation method of the mesoporous zirconium phosphate using an aqueous solution of ammonium metavanadate (Aldrich). The mixture was rotaevaporated until complete dryness. After that, these materials were dried overnight in an oven at 100 °C. Finally the samples were calcined at 500 °C for 6 h.

For comparison, a pure V_2O_5 catalyst has been prepared by calcination in air at 500 °C for 2 h from ammonium metavanadate.

2.2. Catalytic tests

Catalytic tests for the partial oxidation of H_2S to sulfur were carried out at atmospheric pressure in a fixed-bed quartz tubular flow reactor, in the 180–260 °C temperature range. The catalyst weight (0.1 g) and a total flow (130 mL min^{-1}) with H_2S/air/He molar ratio of 1.2/5.0/93.8 have been used for catalytic tests.

Analysis of reactants and reaction products was carried out on-line using gas chromatography and two different chromatographic columns (Molecular Sieve 5A and Porapak T).

2.3. Catalyst characterization

Catalyst surface areas were determined by multi point N_2 adsorption at −196 °C, and data were treated in accordance with the BET method. The textural properties of all samples were determined by nitrogen isotherms at liquid N_2 temperature, using a Micromeritics ASAP 2010 apparatus (static volumetric technique). Before determination of adsorption–desorption isotherms the samples (0.2 g) were outgassed for 16 h at 400 °C under vacuum. The specific surface area (S_{BET}) was evaluated by 2-parameter linear BET plot in the range P/P_0 0.01–0.2. The total pore volume (Vpore) was determined from the amount adsorbed at relative pressure of 0.995. Mean pore size was evaluated with the BJH method applied on the adsorption isotherm branch.

X-ray diffraction patterns were collected in an Enraf Nonius PSD120 diffractometer with a monochromatic Cu $K\alpha_1$ source operated at 40 kV and 30 mA. Phases were identified by matching experimental patterns to the JCPDS powder diffraction file.

Raman spectra were recorded in ambient conditions using a Renishaw system 1000 "in via" attached to a microscope. An argon ion laser (785 nm) was used as the excitation source and was typically operated at a power of 20 mW. Spectra were collected using a backscattering geometry with a 180° angle between the illuminating and the collected radiation.

Diffuse reflectance UV–vis (DR–UV–vis) spectra were recorded on a Cary 5 equipped with a Praying Mantis attachment from Harric.

Temperature-programmed reduction (TPR) was carried out in a Micromeritics Autochem 2910 equipped with a TCD detector. The reducing gas used in all experiments was 10% H_2 in Ar, with a flow rate of 50 mL min^{-1}. The temperature range explored was from room temperature to 800 °C. The heating rate was maintained at 10 °C min^{-1} for all samples whilst the sample mass was varied depending on the sample under study. Details of specific conditions are given with the TPR profiles.

Infrared spectra of adsorbed pyridine were obtained in a Nicolet 710 FTIR spectrophotometer. Wafers of 10 mg cm^{-2} were mounted in a pyrex vacuum cell fitted with CaF_2 windows. The samples were pre-treated overnight at 400 °C and then cooled at room temperature (rt) to obtain the original IR spectra. Then, pyridine was admitted at room temperature, degassed at 150 °C for 1 h in order to remove the fraction physisorbed, and the spectra registered at room temperature. Pyridine was also desorbed at 250 °C.

X-ray photoelectron spectra were collected using a Physical Electronics PHI 5700 spectrometer with non monochromatic Mg Kα radiation (300W, 15 kV, 1253.6 eV) for the analysis of core level signals of C1*s*, O1*s*, Si 2*p*, P 2*p*, Zr 3*d*, V 2*p* and S 2*p*. Spectra of powdered samples were recorded with the constant pass energy values at 29.35 eV, using a 720 μm diameter analysis area. Under these conditions, the Au $4f_{7/2}$ line was recorded with 1.16 eV FWHM at a binding energy of 84.0 eV. The spectrometer energy scale was calibrated by using the Cu $2p_{3/2}$, Ag $3d_{5/2}$ and Au $4f_{7/2}$ photoelectron lines at 932.7, 368.3 and 84.0 eV, respectively. During data processing of the XPS spectra, binding energy values were referenced to the C1*s* peak (284.8 eV) from the adventitious contamination layer. The PHI ACCESS ESCA-V6.0 F software package was used for acquisition and data analysis. A Shirley-type background was subtracted from the signals. Recorded spectra were always fitted using Gauss–Lorentz curves, in order to determine the binding energy of the different element core levels more accurately. The error in BE was estimated to be ca. 0.1 eV. Short acquisition time of 10 min was first used to examine C1*s*, V 2*p* regions in order to avoid, as much as possible, photo-reduction of V^{5+} species. Satellite subtraction was always performed to study the V 2*p* and S 2p regions.

3. Results and discussion

3.1. Catalytic test in the selective oxidation of H_2S to sulfur

Fig. 2 shows the variation of the conversion of H_2S (Fig. 2a) and the selectivity to SO_2 (Fig. 2b) with the time on stream (TOS) during

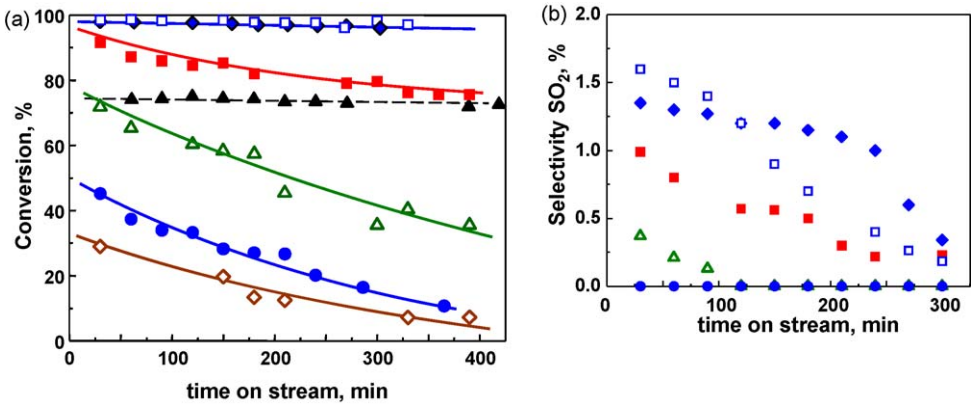

Fig. 2. Variation of the H_2S conversion (a) and the selectivity to SO_2 (b) with the time on stream (TOS) obtained over MZP-supported vanadium oxide catalysts. Reaction conditions: 0.1 g of catalyst; total flow of 130 mL min^{-1}; H_2S/air/He molar ratio of 1.2/5.0/93.8 (i.e. H_2S/O_2 ratio of 1/0.9); W/F = 31.2 g_{cat} h^{-1} mol_{H2S}^{-1}. Symbols: 0V-MZP (◇) 2V-MZP (●); 4V-MZP (△); 8V-MZP (■); 12V-MZP (□); 16V-MZP (◆); V_2O_5 (▲).

the oxidation of H_2S over supported vanadia catalysts at 200 °C. For comparison, the catalytic results achieved over pure V_2O_5 and V-free support have been also included. In all cases, sulfur and water were the only reaction products, while SO_2 was only observed as minority (selectivities lower than 3%) in the first minutes of these experiments (Fig. 2b). It can be seen how the conversion of H_2S increases with the vanadium content.

Initial catalyst decay during the first hours of each experiment can be observed on catalysts with low V-loadings. However, no appreciable catalytic activity decay was observed for samples with V-content higher than 12wt% of V-atoms as well as over pure V_2O_5. In this way, catalytic results achieved at W/F = 32.1 g_{cat} h mol_{H2S}^{-1} shows an initial H_2S conversion of ca. 98% over samples 12V-MZP and 16V-MZP after 6 h of time on stream. This catalytic activity is higher than that observed over pure V_2O_5 (ca. 75%).

Table 1 shows comparatively the space time yield (STY) for sulfur formation achieved at a TOS of 0.5 h obtained on catalysts with different V-loading. It can be seen that a space time yield (STY) of ca. 1000 g_S h^{-1} kg_{cat}^{-1} can be achieved over sample 12V-MZP, while lower productivities have been observed for samples with lower or higher V-loading. Accordingly, the conversion of H_2S increases with the V-loading of catalysts, presenting a maximum over the catalysts with a V-loading of 12wt%. In all cases, no considerable emission of SO_2 has been detected at high time on streams.

In order to comparatively study the catalytic behaviour of stabilized catalysts, a second series of experiments were carried out after a catalyst pre-treatment at 250 °C with diluted H_2S (1% in helium) and a total flow of 125 mL min^{-1} during 4 h. The catalytic results for catalysts containing from 4 to 16wt% of V-atoms in the reaction temperature range of 180–260 °C are shown in Fig. 3. The hydrogen sulfide conversion increases with the reaction temperature and no catalyst deactivation was observed after these catalytic tests. This trend is similar to that previously observed over supported vanadia catalysts [7–20]. On the other hand, the catalytic activity increases initially with the V-loading presenting a maximum for the catalysts with a 12wt% of V-atoms. These results indicate that V-sites are active and selective for the oxidation of hydrogen sulfide in both fresh and pre-treated catalysts. However, the formation of SO_2 seems to be favoured when the reaction is carried out at high reaction temperature (Fig. 3b).

3.2. Characterization of fresh catalysts

Table 1 shows comparatively some characteristics of fresh catalysts. It can be seen that the surface area and the pore volume of catalyst decrease when increasing the vanadium loading, as a consequence of a partial loss of the mesoporous character with the incorporation of vanadium. In fact, the low angle reflection line d_{001} of MZP material disappears with the incorporation of high V-contents.

Fig. 4 shows the XRD patterns of calcined catalysts before (Fig. 4A) and after the catalytic tests (Fig. 4B). No crystalline phases have been observed for catalysts with V-loading lower than 4wt% of V-atoms.

For fresh catalysts with a higher V-loading it can be seen the appearance of new peaks at 2θ = 15.3, 18.6, 20.3, 21.5, 23.6, 26.2, 30.2, 31.2, 34.3 and 35.5, 44.5, 47.3, 49.0, 51.2, 53.5 and 57.3° (the intensity of these peaks increase with the increase of the V-loading). These results suggest the presence of V_2O_5 [JCPDS: 41–1426] (with diffraction peaks 2θ = 15.3, 20.3, 26.2, 31.2, 34.3, 47.3°) in addition to ZrP_2O_7 [JCPDS: 85–896] (diffraction peaks at 2θ = 18.6, 21.5, 24.1, 26.2 and 30.2°), the formation of both favoured on catalysts with high V-contents.

Table 1
Characteristics of supported vanadium oxide catalysts.

Sample	V-content (wt%)[a]	S_{BET} (m^2 g^{-1})	Pore volume (cm^3 g^{-1})	TPR results[b]		H_2S oxidation
				TCM (°C)	H_2-uptake (10^4 mol_{H2} g_{cat}^{-1})	STY (g_S h^{-1} kg_{cat}^{-1})[c]
0V-MZP	0.0	556	0.54		0	218
2V-MZP	2.1	212	0.50	550	2.3	490
4V-MZP	4.1	158	0.56	550	6.9	785
8V-MZP	8.4	151	0.49	550	16.1	986
12V-MZP	12.7	89.8	0.43	550	25.2	1054
16V-MZP	16.9	35.0	0.30	560	42.0	1054
V_2O_5	56.0	3.0	–	619	n.d.	806

[a] V-content in calcined samples in wt% of V-atoms.
[b] Temperature of maximum hydrogen consumption (TCM) and H_2-uptake (in mol_{H2} g^{-1}) achieved during the TPR results; n.d. = not determined.
[c] Space time yield (STY) of sulfur formation, in g_S h^{-1} kg_{cat}^{-1}, calculated after 0.5 h of time on stream. Reaction conditions as in Fig. 2.

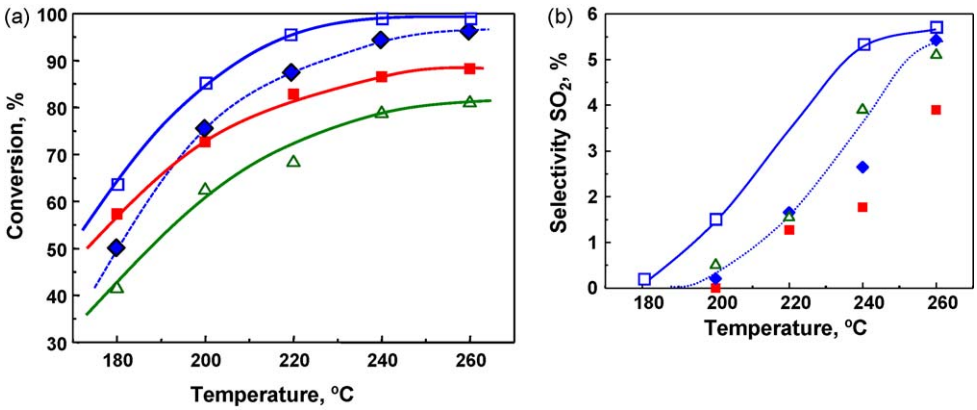

Fig. 3. Variation of the H_2S conversion (a) and the selectivity to SO_2 (b) with the reaction temperature of pre-treated samples. *Pre-treatment conditions*: temperature = 250 °C (4 h); total flow of 125 mL min^{-1} of a 1% of H_2S/He; weight of catalyst = 0.1 g. *Reaction conditions*: 0.1 g of catalyst; total flow of 130 mL min^{-1}; H_2S/air/He molar ratio of 1.2/5.0/93.8 (i.e. O_2/H_2S ratio of 0.85); W/F = 31.2 g_{cat} h^{-1} mol_{H2S}^{-1}. Symbols: 4V-MZP (△); 8V-MZP (■); 12V-MZP (□); 16V-MZP (◆).

We must indicate that it has been reported that mesoporous zirconium phosphate can be partially destroyed during the calcination step [21]. Moreover, the results presented here suggest that this partial destruction of the mesoporous structure (with the formation of ZrP_2O_7) could be favoured the presence of high V-loading.

Raman spectra of catalysts in ambient conditions are presented in Fig. 5. The calcined samples show bands at 998, 706, 530, 489, 410, 305, 289, 203 and 159 cm^{-1} (Fig. 5A). These bands refer to the vibrational modes of crystalline V_2O_5 [22,23]. In addition to these, a shoulder at 1024 cm^{-1} is clearly observed in samples with a high V-loading, which is associated to terminal V=O bond of an amorphous cluster [24]. However, the fact that the Raman bands corresponding to crystalline V_2O_5 are also observed in samples with low V-loadings while V_2O_5 crystal are not observed by the XRD suggests the formation of crystalline phase with low crystal size in samples with V-loading lower than 4wt%.

Diffuse reflectance UV–vis spectra of catalysts are shown in Fig. 6. The bands observed in the range of 200–500 nm arise from low-energy O^{2-} to V^{5+} charge-transfer while the d–d transition of V^{4+} species occur at higher energies (600–800 nm) [25,26]. For the calcined catalyst with the lowest V-loading (2.0wt%) only one main band centred at ca. 265 nm is observed (Fig. 6A, spectrum a). However, an intense broad band at 260–280 nm with a shoulder at 377 nm, which increases when increasing V-loading can be observed for catalysts with V-loadings higher than 4wt% (Fig. 6A, spectra b, c and d). The absorption band at 270–290 nm indicates the presence of isolated tetrahedral V^{5+} while bands at 245 and 370 nm indicate the presence of associated vanadium species. In addition to those, a third band around 465 nm is clearly observed in the sample with a V-loading higher than 8wt%. This band is related to the presence of "bulk-type" polymeric V_2O_5-like vanadium species.

Pyridine adsorption was followed by infrared spectroscopy to identify the number and nature of acid sites. Fig. 7 shows the FTIR spectra of pyridine adsorbed on MZP-supported catalysts after evacuation at 150 °C. The bands at 1450, 1492 and 1622 cm^{-1} are associated to pyridine coordinated to Lewis acid sites, while bands at 1540 and 1638 cm^{-1} are related to pyridinium cations in Brönsted acid sites [27]. The intensity of these bands decreases when increasing the V-loading suggesting the partial elimination of acid sites due to the support. On the other hand, the relatively low acid strength of these acid sites is evidenced by the partial disappearance of these bands upon desorption at 250 °C (spectra not shown), suggesting that only a part of pyridine is retained on Lewis acid sites.

Fig. 8 depicts the H_2–TPR profile of supported vanadia catalysts from room temperature to 800 °C. The studied catalysts show one broad peak, which is related to the reduction of the V^{5+} to V^{3+}. The catalyst with low V-loading (2.0wt%) presents the reduction band at ca. 540 °C while in the rest of the samples the band is observed at *ca.* 550 °C. Except in the case of the sample with the lower V-loading, the reduction peak can be related to the presence of V_2O_5 crystallites with relatively small crystal size [28,29]. In this way, the high reduction temperature observed in the TPR pattern of pure V_2O_5 (Fig. 8 pattern d) is probably due to the low accessibility of H_2 to the lattice vanadium atoms in the V_2O_5 bulk [29], as a consequence of the higher crystal size in this sample. On the other

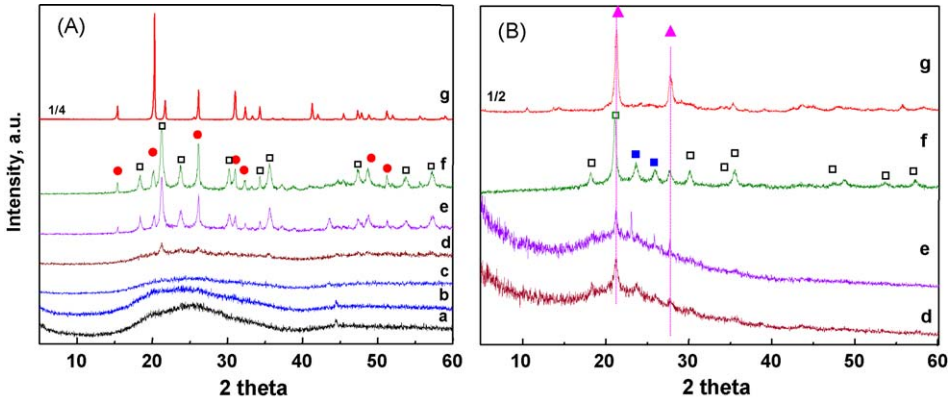

Fig. 4. XRD patterns of MZP-supported vanadium oxide catalysts before (A) and after (B) the catalytic test: (a) 0V-MZP; (b) 2V-MZP; (c) 4V-MZP; (d) 8V-MZP; (e) 12V-MZP; (f) 16V-MZP; (g) V_2O_5. Symbols: V_2O_5 (●); ZrP_2O_7 (□); V_4O_9 (▲); elemental sulfur (■). Used catalysts where those obtained after experiments presented in Fig. 2.

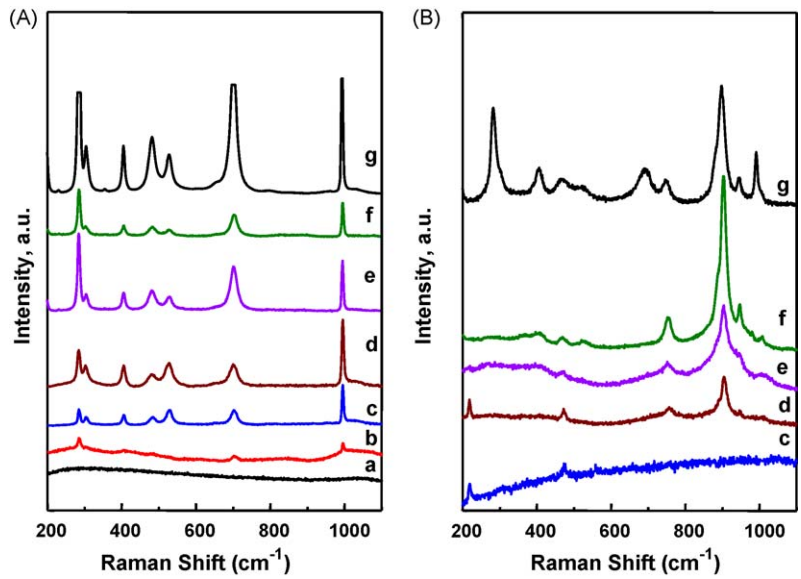

Fig. 5. Raman spectra of MZP-supported vanadium oxide catalysts before (A) and after (B) the catalytic test: (a) 0V-MZP; (b) 2V-MZP; (c) 4V-MZP; (d) 8V-MZP; (e) 12V-MZP; (f) 16V-MZP; (g) V_2O_5. Used catalysts where those obtained after experiments presented in Fig. 2.

hand, an average oxidation state of ca. +4 can be deduced from the H_2-uptake observed during the TPR of sample 2V-MZP. Moreover, an average oxidation state of ca. +3 can be proposed for samples with higher V-contents after the TPR experiments.

Table 2 shows the XPS results of fresh catalysts. Concerning the composition of the fresh catalysts, the surface vanadium content of sample 8VMZP is slightly higher than that of sample 4VMZP in spite of the higher vanadium content of sample 8VMZP. However, as expected, sample 12VMZP has a surface vanadium content triple than that found in sample 4VMZP. This means that with a low amount of vanadium, most part of vanadium species are inside the pore and a small proportion is at the external surface of the catalyst. When more vanadium is added (sample 8VMZP), these additional vanadium species are also located into the pores of the support. But with a further addition of vanadium, the vanadium oxides could be mainly covering the external surface of the catalyst (sample 12VMZP), which should also be favoured by the decrease in the catalyst surface area. The binding energy values of the constituent elements of the support are not modified upon the incorporation of vanadium species (see Table 2). The core level V 2*p* signal shows interesting facts. With a low V-loading (sample 4VMZP) the V $2p_{3/2}$ signal can be decomposed in two contributions at 518.0 and 516.5 eV assigned to V^{5+} and V^{4+} [30,31], respectively, and where the proportion of V^{4+} is relatively high (35%). Upon the incorporation of more vanadium, the proportion of V^{4+} dramatically decreases, being 7% for sample 12VMZP. The high proportion V^{4+} at the surface of sample 4VMZP may be due to several reasons such as photoreduction or thermal reduction of dispersed vanadia. These effects are moderated with higher contents of vanadium.

Typical bulk atomic ratio composition, determined by EDX analysis, for mesoporous zirconium phosphate heterostructure of Zr P and Si as more representative elements, is 1:2.21:6.31, respectively. The found P/Zr molar ratio (2.2) is close to the theoretical value of 2.0. This indicates that the chemical composition of the layer of zirconium phosphate is not modified by the silica galleries formation into interlayer space. Also, the Si/P molar ratio is 2.85 close to the theoretical value of 3.0 (the value of the TEOS/P molar ratio added) which indicates that the hydrolysis and condensation of silica precursors is carried out massively. This bulk composition value of MZP used as support is in the range of the

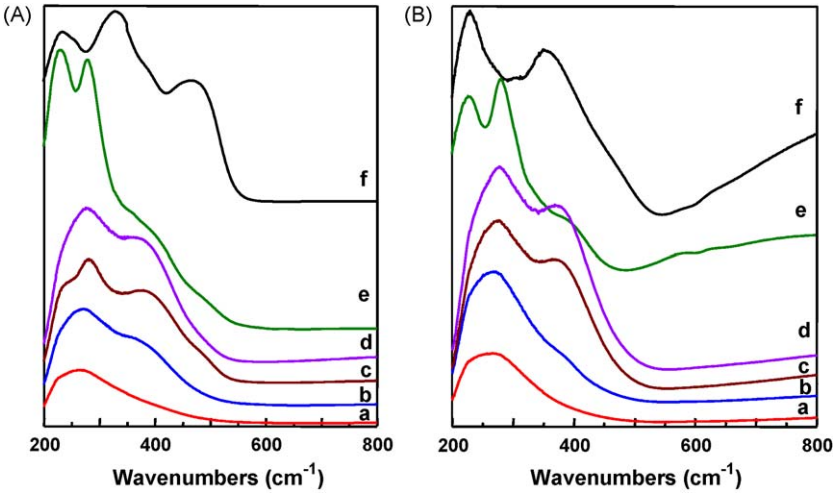

Fig. 6. DR–UV–vis spectra of MZP-supported vanadium oxide catalysts before (A) and after (B) the catalytic test: (a) 2V-MZP; (b) 4V-MZP; (c) 8V-MZP; (d) 12V-MZP; (e) 16V-MZP; (f) V_2O_5. Used catalysts where those obtained after experiments presented in Fig. 2.

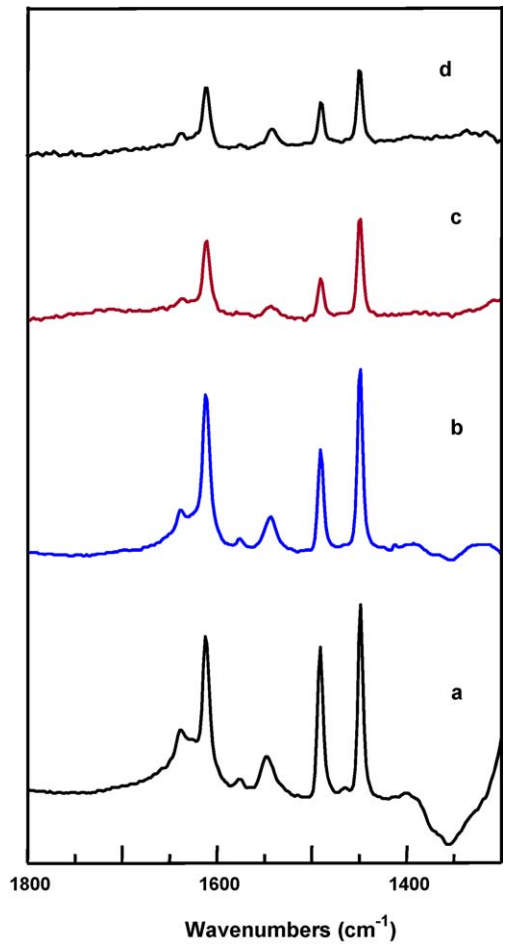

Fig. 7. FTIR spectra of adsorbed pyridine on MZP-supported vanadium oxide catalysts: (a) 0V-MZP; (b) 4V-MZP; (c) 8V-MZP; (d) 12V-MZP. After evacuation at 150 °C.

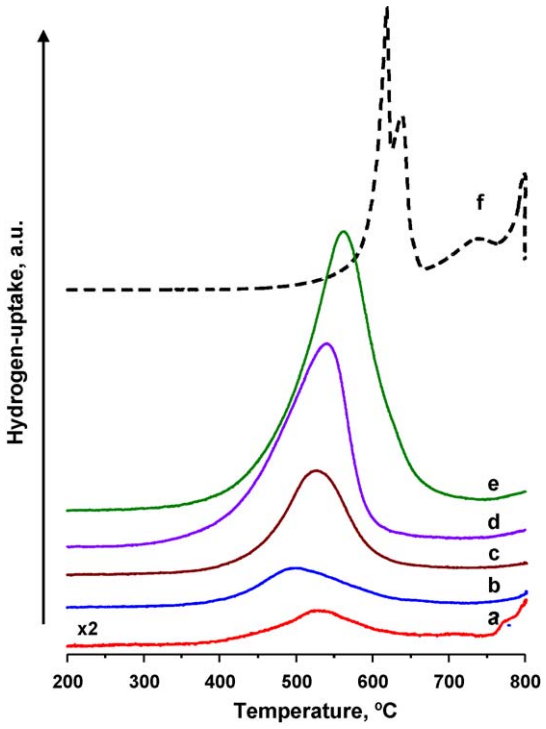

Fig. 8. TPR patterns of results on MZP-supported vanadium oxide catalyst: (a) 2V-MZP; (b) 4V-MZP; (c) 8V-MZP; (d) 12V-MZP; (e) 16V-MZP; (f) V_2O_5.

surface composition obtained by XPS indicating the homogeneity of this material.

3.3. Characterization of used catalysts

In all cases, the catalysts have been also characterized after the catalytic tests (in which the samples were recorded after a time on stream of ca. 6 h, see Fig. 2). The corresponding XRD patterns of used catalysts are shown in Fig. 4B. It can be seen the presence of a diffraction peak at $2\theta = 21.5^\circ$ related to the presence of crystalline ZrP_2O_7. In addition, other peaks with low intensities can be observed at $2\theta = 18.3, 23.8, 27.6, 35.8$ and 43.6°. When comparing to those achieved from fresh catalysts (Fig. 4 A), it can be concluded the disappearance of V_2O_5 and the formation of V_4O_9 [JCPDS: 23–720], which increase with the V-loading, for catalysts after the catalytic test. A similar behaviour can also be concluded when using pure V_2O_5 as catalyst, in which the preferential formation of V_4O_9 is clearly observed. However the presence of sulfur crystals [JCPDS: 8–247] (peak at $2\theta = 23.1^\circ$), as minority, is only observed on catalysts with low V-loading.

The Raman spectra of used catalysts (Fig. 5 B) show a drastic change with respect to those of fresh catalysts (Fig. 5 A). Thus, bands at 920, 900 (with a shoulder at 886 cm^{-1}) and 720 cm^{-1} are observed in used catalysts, while the main features of the bands related to V_2O_5 crystallites (bands at 998, 706, 530, 489, 410, 305, 289, 203 and 159 cm^{-1}) are only observed as minorities in the case of used V_2O_5 catalysts. Nilsson et al. [32], reported bands at 900 and 720 cm^{-1} in addition to a shoulder at 886 cm^{-1} related to V_4O_9, which was formed during the propane ammoxidation over V_2O_5. Accordingly, V_4O_9 could also be formed in our catalyst during the oxidation of H_2S, probably as a consequence of a low reoxidation of catalyst in the reaction conditions used here. In this way, we can indicate that both V_2O_5 (bands at 998, 706, 530, 489, 410, 305, 289, 203 and 159 cm^{-1}) and V_4O_9 are observed in the case of pure V_2O_5 sample (Fig. 5B, spectrum g). This indicates that only a part of V^{5+} species were reduced after a time of stream of 6 h. Although these results are not completely conclusive about the presence of V_4O_9 in working catalysts recent results carried out

Table 2
XPS results of fresh catalysts.

Sample	Surface composition	Core level binding energy (eV)				
	O/Si/P/Zr/V atomic ratio	O1*s*	Si 2*p*	P 2*p*	Zr $3d_{5/2}$	V $2p_{3/2}$
0V-MZP	71.90/17.48/6.70/3.45/0.00	532. 2	102.8	133.5	183.1	–
4V-MZP	71.85/17.35/6.24/3.30/0.94	532.1	102.8	133.6	183.1	518.0 (65%) 516.5 (35%)
8V-MZP	70.54/17.31/6.60/3.35/2.02	531.9	102.8	133.5	182.9	517.8 (75%) 516.5 (25%)
12V-MZP	71.43/16.54/5.77/2.94/3.11	532.0	102.8	133.4	183.1	517.8 (93%) 516.5 (7%)

by our group in operando XAS confirm the formation of this crystalline phase during the reaction on similar catalysts [33].

The assignation of the band at 920 cm^{-1} is at the moment not clear [34–36]. This could be related to V=O stretching vibration of dioxo units in vanadate chains [34] or to the presence of a $O_dV(OH)2–Ob–M$ moiety at the support surface [35]. However, it cannot be completely ruled out the presence of VO_2^+ in ribbon like moieties [36].

Moreover, we must indicate the absence of VO_2 crystals in used catalysts, which is characterized by the presence of a band at 614 cm^{-1} [37].

On the other hand, bands at 218 and 472 cm^{-1} are observed for samples with a V-loading of 2.0 and 4.0 wt% of V-atoms, while their intensities are very low in the case of sample 8V-MZP (Fig. 5B, spectra c to e). However, these bands are not observed in the case of the sample with higher V-loading. The band at 218 cm^{-1} (with a low intense band at 150 cm^{-1}) can be assigned to S–S–S bending vibration, while the band at 472 cm^{-1} can be related to S–S stretching of polymeric sulfur species adsorbed at multilayer level [38]. However, no bands related to the formation of vanadyl sulfate (bands at 1060 and 984 cm^{-1} [39]) have been observed.

These results suggest that the deposition of sulfur on the catalyst surface is favoured in catalysts with low V-loading, while it is disfavoured in catalysts with high V-loading. In other words, the deposition of sulfur could be favoured on catalysts presenting dispersed vanadia species and/or acid sites in the surface of the vanadium-free support but not in the catalysts presenting only V_2O_5 crystallites and low surface areas.

In the case of the core level S 2p signal (see Fig. 9), there are two peaks with S $2p_{3/2}$ values at 163.2–163.6 eV assigned to elemental sulfur [31,40], and at 168.3–168.4 eV assigned to sulfate [31], where the percentage of elemental sulfur is always higher than that of sulfate. These percentages hardly vary with the vanadium loading. On the other hand, the fact that sulfate is observed by XPS but it is not observed by Raman suggests that the amount of this is low and they are only deposited on the surface of catalyst.

Concerning the core level V 2p signal, the V $2p_{3/2}$ signal can be decomposed in two contributions at 517.5 eV and 516.3 eV, assigned to V^{5+} and V^{4+}, respectively [30] as in the case of the fresh samples. However, now the percentages of V^{4+} are always the same independent of the vanadium loading, in agreement to previous results [13,14]. This can be attributed to the presence on the surface of V_4O_9, in all the used catalysts with a theoretical V^{5+}/V^{4+} ratio of ca. 1. However, a partial surface oxidation as a consequence of the regeneration of the catalyst surface after some days in contact with air cannot be completely ruled out, although it should be low.

3.4. General remarks

In the experimental conditions at which the different solids were assayed to study the partial oxidation of H_2S to sulfur V-containing samples are active and very selective (>95%), the catalytic activity increasing with the V-loading. However, the V-free support present a low catalytic activity, Accordingly both dispersed vanadium species (in samples with low V-content) and V_2O_5 crystallites (in catalysts with high V-content) seems to be active and selective in the partial oxidation of hydrogen sulfide to sulfur, although the catalytic activity of V-sites depend on the V-loading.

Table 1 shows the space time yield, STY, calculated after 0.5 h of time on stream. A maximum in the formation of sulfur is observed for catalysts with V-content of 12wt%, which present mainly V_2O_5 crystallites. It is clear that catalysts presenting V_2O_5 crystallites must have a low dispersion and accessibility of V-sites than those presenting only isolated vanadium species. However, the formation of V_2O_5 crystallites with crystal sizes lower than that achieved in pure V_2O_5. This can explain the higher catalytic activity of supported catalysts and the higher reducibility of V-species in supported catalysts to those observed in pure V_2O_5.

In addition, not only the catalytic activity and the space time yield STY (Table 1) but also the catalyst stability increases with the V-loading. Thus, important catalytic activity decay is clearly observed for the samples with the lower V-content, while the catalysts are practically stable for V-loading higher than 8wt% (Fig. 2). For this reason, and in order to evaluate the nature of V-sites before and after the catalytic tests, a characterization of catalysts after the catalytic test has been also carried out.

According to the XRD, Raman and XPS results, the vanadium species are partially reduced during the catalytic tests. When comparing the catalysts with different V-contents it can be observed that the ratio V^{5+}/V^{4+} is maintained constant for all the studied catalysts. However, this fact can be explained taking into account that in all used catalysts, V_4O_9 crystals are clearly observed in those presenting V_2O_5 crystals before the catalytic tests.

It is clear that the appearance of V_4O_9 in used catalysts, which is determined by ex situ characterization technique, confirm only a reduction of V-sites during the reaction. However, the appearance of V_4O_9 in used catalysts could be a consequence of the reduction (and the partially reoxidation of the sample in ambient conditions

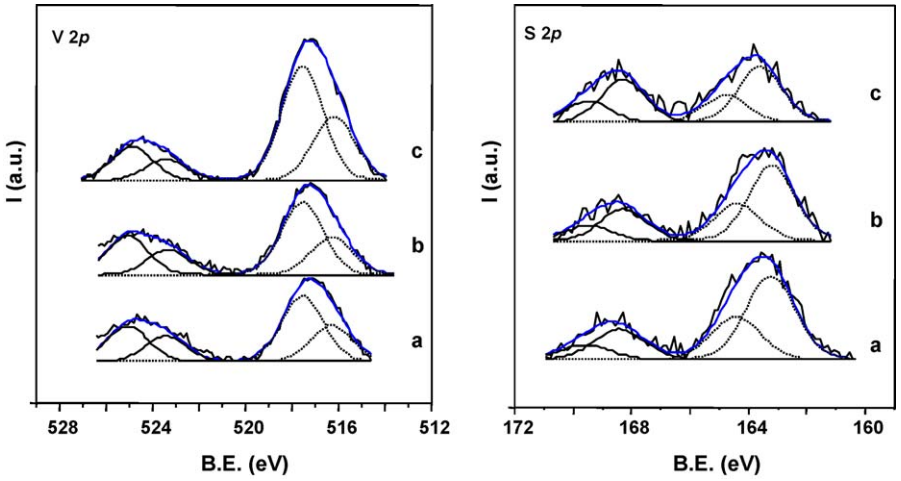

Fig. 9. V 2*p* and S *p* core level spectra for MZP-supported vanadium oxide catalysts after the catalytic test. Samples: (a) 4V-MZP; (b) 8V-MZP; (c) 12V-MZP. Used catalysts where those obtained after experiments presented in Fig. 2.

Table 3
XPS results of used catalysts.

Sample	Surface composition	Core level binding energy (eV)					
	O/Si/P/Zr/V/S atomic ratio	O1*s*	P 2*p*	Si 2*p*	Zr $3d_{5/2}$	V $2p_{3/2}$	S $2p_{3/2}$
4V-MZP	68.14/17.38/7.32/3.91/1.14/1.10	532.1	133.6	102.8	183.1	517.5 (64%) 516.3 (36%)	163.2 (72%) 168.4 (28%)
8V-MZP	68.38/17.11/7.46/3.94/2.02/1.09	531.9	133.5	102.8	182.9	517.5 (66%) 516.3 (34%)	163.2 (70%) 168.3 (30%)
12V-MZP	68.50/16.79/6.90/3.70/3.45/0.66	532.0	133.4	102.8	183.1	517.5 (64%) 516.3 (36%)	163.6 (66%) 168.3 (34%)

during the characterization step). However, recent result of our group working in operando conditions with this type of catalysts, confirm that V_4O_9 is mainly formed during the partial oxidation of V-supported vanadium oxides catalysts [33]. Accordingly, V_4O_9 could be proposed as active and selective phase in the hydrogen sulfide oxidation to sulfur over these catalysts. Note that V_4O_9 has been also reported to be formed during the propane ammoxidation over V_2O_5, as a consequence of a partial reduction of V_2O_5 during the ammoxidation reaction [32].

V_4O_9 seems to be stable in our reaction conditions as a consequence of a low reoxidation of catalyst when working at relatively low reaction temperature (200 °C). In this way, we can notice that no catalyst's decay of sample 12 V-MZP has been observed after 6 h (working at 200 °C, see Fig. 2) in which V_4O_9 was observed after this catalytic experiment. Neither VO_2 nor $VOSO_4$ have been observed in our case. This probably is due to the minor reductive character of the reaction mixture [6] and the lower reaction temperature [17].

The orthorhombic V_4O_9 is characterized by the presence of V^{5+}–O–V^{4+} pairs, with vanadium atoms exclusively in square-pyramidal coordination with oxygen [41,42]. We must indicate that this crystalline structure can be easily formed by a partial reduction of V_2O_5 [43,44], but it can be also easily oxidized to V_2O_5 in the presence of O_2 at 200–250 °C [44]. In addition, one particularity of V_4O_9 is its relative stability and facility to transport lattice oxygen from the bulk to the surface, which could favour a redox mechanism in the selective oxidation of H_2S to elemental sulfur.

We must indicate that V_4O_9 can be achieved by reducing V_2O_5 single crystals at 250 °C for 50 h in a sulfur atmosphere, although prolonging the treatment led to the formation of VO_2 [45]. Thus, a partial reduction of V_2O_5 to V_4O_9 seems to be more favoured at 200 °C in the reaction conditions used in this study.

On the other hand, the catalyst decay in samples with low V-loading could be related to the low ability to form stable V^{4+}-species, while this occurs easily during the formation of V_4O_9 from V_2O_5 crystallites in catalysts with high V-contents. However, other factor should be also considered in this case. Thus, sulfur and sulfate species are observed on the surface of used catalysts (Table 3), while sulfur crystals are observed by Raman and XRD. Since the amount of S on the catalyst surface decreases when increasing the V-loading one could consider that V-free sites of the mesoporous support could be involved in the incorporation of sulfur on the catalyst surface.

The characterization results of calcined samples indicate that the support is partially transformed from the Mesoporous Zirconium Phosphate Heterostructure to ZrP_2O_7 when increasing the V-loading. This loss of the surface area of the support and the appearance of ZrP_2O_7 could favour the disappearance of acid sites (as determined by FTIR of pyridine adsorption, Fig. 7), which could also favour a lower deposition of sulfur on the catalyst surface (as determined by XPS, Table 3) in samples with high V-loading. Accordingly, catalysts with low number of acid sites should be preferred in order to decrease the sulfur adsorption of the catalyst. However, these aspects should also be studied in the future in order to adequately address the modifications occurring in the catalysts during the catalytic tests.

In conclusion, vanadium oxide supported on mesoporous zirconium phosphate is active and selective in the partial oxidation of H_2S to elemental sulfur, although both catalytic behaviour and catalyst stability strongly depend on the V-loading. Catalysts with low V-loading with both isolated V^{5+} species and V_2O_5 crystallites are less active and show high catalyst decay than pure V_2O_5. However, catalysts with high V-loading, in which V_2O_5 crystallites are mainly observed, show a catalytic activity and stability higher than pure V_2O_5. So, apparently V_2O_5 could be proposed as the active and selective phase in this reaction. However, the characterization results of tested catalysts have demonstrated the formation of partially reduced crystalline phase, V_4O_9-like, during the catalytic test. This has been recently confirmed by carrying out the catalyst characterization in operando conditions [33]. Accordingly, it can be concluded that: (i) a slow catalyst reoxidation occurs in theses catalysts in the reaction conditions used in this study; (ii) the partially reduced phase is active and selective in the partial oxidation of H_2S.

In addition, if SO_2 is initially observed in the first minutes of the reaction, it is practically not observed (the selectivity to sulfur is >99%) at high time on stream when working at 200 °C. Moreover, although the selectivity to SO_2 increases (up to ca. 3–5%) when increasing the reaction temperature.

Accordingly, V_4O_9 (which is observed only in catalysts studied at 200 °C) seems to be the active and selective crystalline phase in the reaction conditions used in this work, i.e. reaction temperature of 200 °C and a H_2S/O_2 ratio of 1.2. However, and according to the redox properties of these materials the nature of crystalline phases formed in this reaction could be change depending on the reaction conditions. So, the redox properties of this catalytic system play an important role in both catalytic behaviour and formation of stable crystalline phases.

Acknowledgments

The authors gratefully acknowledge financial support from CICYT, Spain (NAN2004-09267-C03-01 and NAN2004-09267-C03-02). MDS thanks a fellowship from the Universidad Politécnica of Valencia.

References

[1] R.E. Kirk, F. Orthmer, J.I. Kroschwitz, M. Howe-Grant, Kirk-Othmer's Enciclopedia of Chemical Technology, John Willey & Sons, New York, 1998.
[2] (a) R. Ketter, N. Liermann, Oil Gas J. 86 (1988) 63;
(b) J.A. Lagas, J. Borsboom, P.H. Berben, Oil Gas J. 86 (1988) 68.
[3] (a) S.W. Chun, J.Y. Jang, D.W. Park, H.Ch. Woo, J.S. Chung, Appl. Catal. B 16 (1998) 235–243;
(b) J.H. Uhm, M.Y. Shin, J. Zhidong, J.S. Chung, Appl. Catal. B 22 (1999) 293–393.
[4] T.N. Mashapa, J.D. Rademan, M.J. Janse van Vuuren, Ind. Eng. Chem. Res. 46 (2007) 6338–6344.
[5] A.A. Davydov, V.I. Marshneva, M.L. Shepotko, Appl. Catal. A 244 (2003) 93–100.
[6] M.Y. Shin, Ch.M. Nam, D.W. Park, J.Sh. Chung, Appl. Catal. A 211 (2001) 213–225.
[7] K.-T. Li, T.-Y. Chien, Catal. Lett. 57 (1999) 77–80.
[8] K.T. Li, M.Y. Hyang, W.D. Cheng, Ind. Eng. Chem. Res. 35 (1996) 621–626.

[9] K.T. Li, Z.-H. Chi, Appl. Catal. B 31 (2001) 173–182.
[10] K.T. Li, Z.-H. Chi, Appl. Catal. A 206 (2001) 197–203.
[11] S. Yasyerly, G. Dogu, T. Dogu, Catal. Today 117 (2006) 271–278.
[12] B.K. D-W-Park, D.-K. Park, H.C. Park, Woo, Appl. Catal. A 223 (2002) 215224.
[13] B.-G. Kim, W.-D. Ju, I. Kim, H.-Ch. Woo, D.-W. Park, Solid State Ion. 172 (2004) 135–138.
[14] S. Yasyerli, G. Dogu, I. Ar, T. Dogu, Chem. Eng. Sci. 59 (2004) 4001–4009.
[15] M.I. Kim, D.W. Park, S.W. Park, X. Yang, J.S. Choi, D.J. Suh, Catal. Today 111 (2006) 212–216.
[16] P. Kalinkin, O. Kovalenko, O. Lapina, D. Kjabibulin, N. Kundo, J. Mol. Catal. A 178 (2002) 173–180.
[17] M.W. Song, M. Kang, K.L. Kim, React. Kinet. Catal. Lett. 78 (2003) 365–371.
[18] K.-T. Li, Ch.-H. Huang, Ind. Eng. Chem. Res. 45 (2006) 7096–7100.
[19] D.-W. Park, B.-H. Byung, W-.D. Ju, M.I. Kim, K.-H. Kim, H.-C. Woo, Kor. J. Chem. Eng. 22 (2005) 190–195;
K.V. Bineesh, D.R. Cho, S.Y. Kim, B.R. Jermy, D.W. Park, Catal. Commun. 9 (2008) 2040–2043.
[20] M.I. Kim, W.D. Ju, K.H. Kim, D.-W. Park, S.S. Hong, Stud. Surf. Sci. Catal. 159 (2006) 225–228.
[21] J. Jiménez-Jiménez, M. Rubio-Alonso, D. Eliche-Quesada, E. Rodríguez-Castellón, A. Jiménez-López, J. Mater. Chem. 15 (2005) 3466–3472.
[22] L. Abello, E. Husson, Y. Repelin, G. Lucazeau, Spectrochm. Acta 39 (1983) 641–651.
[23] M.D. Argile, K. Chen, A.T. Bell, E. Iglesia, J. Catal. 208 (2002) 139–149.
[24] S.H. Lee, H.M. Cheong, M.J. Seong, P. Liu, C. Edwin, A. Mascarenthas, J. Roland, S.K. Deb, Solid State Ion. 165 (2003) 111–116.
[25] V.R. Porter, W.B. White, R. Roy, J. Solid State Chem. 4 (1972) 250–259.
[26] Xingtao Gao, I.E. Wachs, J. Phys. Chem. B 104 (2000) 1261–1268.
[27] J. Le Bars, J.C. Vedrine, A. Auroux, S. Trautmant, M. Baerns, Appl. Catal. A 119 (1994) 341–354.
[28] T. Blasco, A. Galli, J.M. López Nieto, F. Trifiró, J. Catal. 169 (1997) 203–211.
[29] B. Solsona, J.M. López Nieto, U. Diaz, Micorp. Mesop. Mater. 94 (2006) 339–347.
[30] L.E. Briand, O.P. Tkachenko, M. Guraya, X. Gao, I.E. Wachs, W. Grünert, J. Phys. Chem. B 108 (2004) 4823–4830.
[31] J.F. Moulder, W.F. Stickle, P.E. Sobol, K.D. Bomben, Standard Spectra for Identification and Interpretation of XPS Data, Perkin Elmer, Eden Prairie, MN, 1992.
[32] R. Nilsson, T. Lindblad, A. Andersson, J. Catal. 148 (1994) 501–513.
[33] J.P. Holgado, M.D. Soriano, J. Jimenez-Jimenez, A. Jimenez-Lopez, P. Concepción, A. Caballero, E. Rodriguez Castellón, J.M. López Nieto, Abstract Third International Congress on Operando Spectroscopy, Rostock-Warnemünde, (2009), pp. P4–07.
[34] G.T. Went, S.T. Oyama, A.T. Bell, J. Phys. Chem. B 94 (1990) 4240.
[35] D.E. Keller, D.C. Koningsberger, B.M. Weckhuysen, J. Phys. Chem. B 110 (2006) 14313.
[36] M. Schraml-Marth, A. Wokaun, M. Pohl, H.-L. Krauss, J. Chem. Soc. Faraday Trans. 87 (1991) 2635.
[37] C. Poccirillo, R. Binions, P. Parkin, Chem. Vap. Deposs. 13 (2007) 145–151.
[38] C. Quijada, F.J. Huerta, E. Morallón, J.L. Vázquez, L.E.A. Berlouis, Electrochim. Acta 45 (2000) 1847–1862.
[39] J.C. Evands, Inorg. Chem. 2 (1963) 372–375.
[40] J. Hrbek, S.Y. Li, J.A. Rodriguez, D.G. van Campen, H.H. Huang, G.-Q. Xu, Chem. Phys. Lett. 267 (1997) 65–71.
[41] K.-A. Wilhelmi, K. Waltersson, Acta Chem. Scand. 24 (1970) 3409–3411.
[42] K.P. Callahan, P.J. Durand, Inorg. Chem. 19 (1980) 3211–3217.
[43] H. Kwon, S. Choi, L.T. Thompson, J. Catal. 184 (1999) 236–246.
[44] J. Haber, M. Witko, R. Tokarz, Appl. Catal. A 157 (1997) 3–22.
[45] G. Grymonprez, L. Fiermans, J. Vennik, Acta Cryst. A 33 (1977) 834–837.